

## Supplementary Information for

# Hydrogen Adsorption in Dehydrated Variants of the Cyano-Bridged Framework Compounds $A_2Zn_3[Fe(CN)_6]_2 \cdot xH_2O$ (A = H, Li, Na, K, Rb)

Steven S. Kaye and Jeffrey R. Long\*

*Department of Chemistry, University of California, Berkeley, California 94720*

*Chem. Commun.*

## Experimental Details

**Gas Adsorption Measurements.** Sample tubes of a known weight were loaded with 100-300 mg of sample and sealed using a transeal. For  $\text{Na}_2\text{Zn}_3[\text{Fe}(\text{CN})_6]_2$ ,  $\text{K}_2\text{Zn}_3[\text{Fe}(\text{CN})_6]_2$ , and  $\text{Rb}_2\text{Zn}_3[\text{Fe}(\text{CN})_6]_2$ , samples were degassed at 95 °C for 24 h on a Micromeritics ASAP 2020 analyzer until the outgas rate was less than 1 mTorr/min. For  $\text{H}_2\text{Zn}_3[\text{Fe}(\text{CN})_6]_2 \cdot 2\text{H}_2\text{O}$ , and  $\text{Li}_2\text{Zn}_3[\text{Fe}(\text{CN})_6]_2 \cdot 2\text{H}_2\text{O}$ , samples were degassed at 40 °C for 48 h. The degassed sample and sample tube were weighed precisely and then transferred back to the analyzer (with the transeal preventing exposure of the sample to air after degassing). The outgas rate was again confirmed to be less than 1 mTorr/min. Measurements were performed either at 77 K in a liquid nitrogen bath, or at 87 K in a liquid argon bath. UHP grade hydrogen, nitrogen, argon, oxygen, and helium (99.999%) were used for all measurements.

### Calculation of the Enthalpy of Adsorption of $\text{H}_2$ .

Enthalpies of adsorption were calculated using a variant of the Clausius-Clapeyron equation:

$$\ln\left(\frac{P_1}{P_2}\right) = \Delta H_{ads} \times \frac{T_2 - T_1}{R \times T_1 \times T_2} \quad (1)$$

where  $P_n$  is the pressure for isotherm  $n$ ,  $T_n$  is the temperature for isotherm  $n$ , and  $R$  is the molar gas constant. This equation can be used to calculate the enthalpy of adsorption as function of the quantity of  $\text{H}_2$  adsorbed. Pressure as a function of the quantity of gas adsorbed was calculated by fitting each isotherm using the Langmuir-Freundlich equation [15]:

$$\frac{Q}{Q_m} = \frac{B \times P^{(1/t)}}{1 + B \times P^{(1/t)}} \quad (2)$$

where  $Q$  is the number of moles of gas adsorbed,  $Q_m$  is the number of moles of gas adsorbed at saturation,  $P$  is the pressure, and  $B$  and  $t$  are fitting constants. In order to obtain the most accurate interpolation between measured data points, only the regions of the isotherm that had been measured at both 77 and 87 K were fitted, as only these regions would be used to calculate the enthalpy of adsorption. Equation 2 was then substituted into equation 1 to give enthalpy of adsorption as function of the quantity of  $\text{H}_2$  adsorbed.

**Other Physical Measurements.** Carbon, hydrogen and nitrogen analyses were obtained from the Microanalytical Laboratory of the University of California, Berkeley. Lithium, sodium, potassium, rubidium, zinc, and iron analyses were obtained from Huffman Laboratories. Thermogravimetric analyses were carried out at a ramp rate of 0.5 °C/mi. using a TA Instruments TGA 2950. Powder x-ray diffraction data was collected using Cu K $\alpha$  ( $\lambda = 1.5406 \text{ \AA}$ ) radiation on a Siemens D5000 diffractometer.

**Table S1.** Unit cell parameters for  $A_2Zn_3[Fe(CN)_6]_2 \cdot xH_2O$  (A = H, Li, Na, K, Rb)

Compound	Space Group	$a$ (Å)	$c$ (Å)
$H_2Zn_3[Fe(CN)_6]_2 \cdot xH_2O$	$R-3c$	12.52(1)	32.828(3)
$Li_2Zn_3[Fe(CN)_6]_2 \cdot xH_2O$	$R-3c$	12.41(1)	33.849(4)
$Na_2Zn_3[Fe(CN)_6]_2 \cdot xH_2O$	$R-3c$	12.427(3)	32.9641(2)
$K_2Zn_3[Fe(CN)_6]_2 \cdot xH_2O$	$R-3c$	12.511(2)	32.0174(2)
$Rb_2Zn_3[Fe(CN)_6]_2 \cdot xH_2O$	$R-3c$	12.479(4)	32.4146(4)

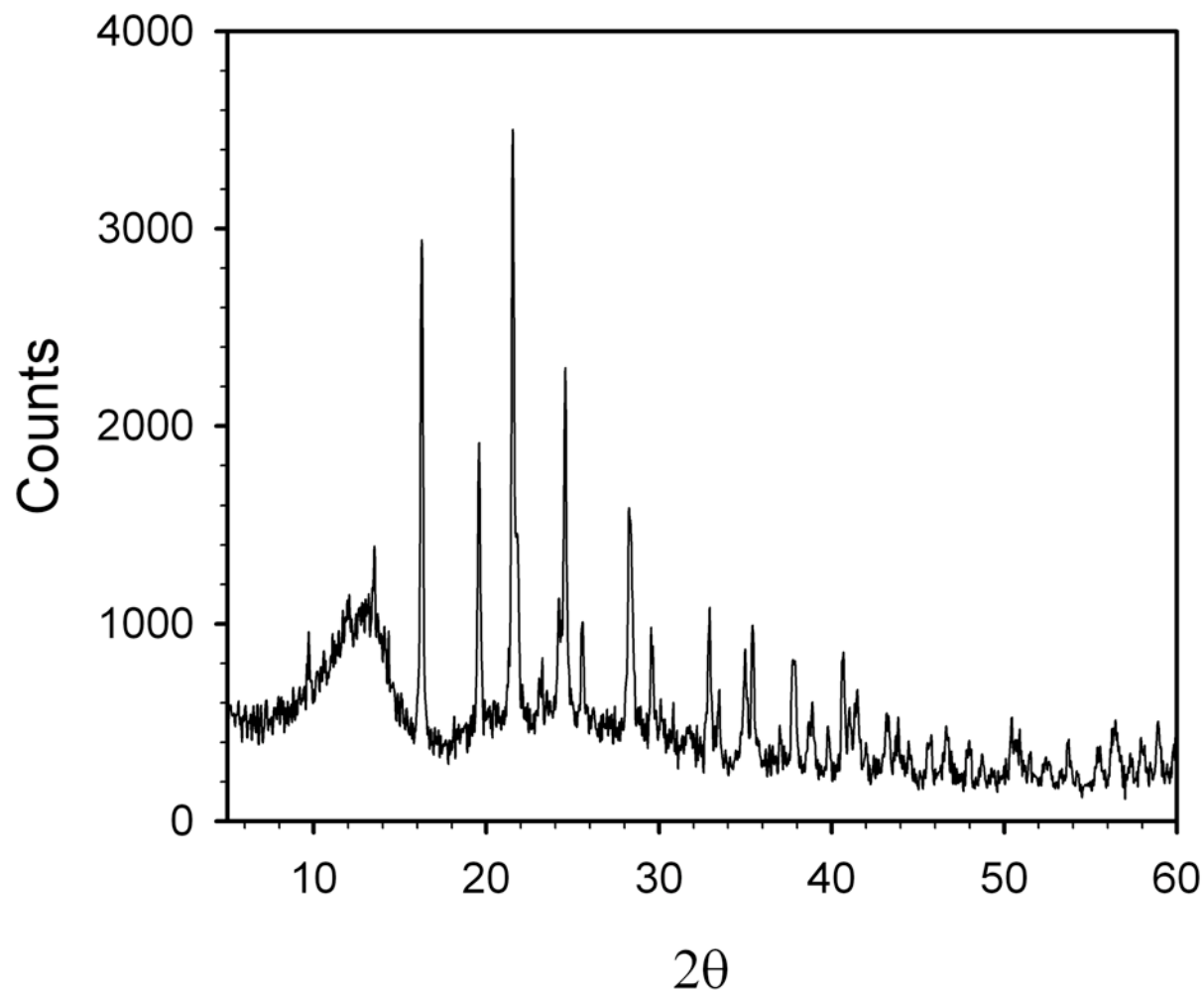


**Fig S1.** X-ray powder diffraction data for  $\text{H}_2\text{Zn}_3[\text{Fe}(\text{CN})_6]_2 \cdot x\text{H}_2\text{O}$ . The broad peak centered at ca.  $13^\circ$  is due to scattering from the sample holder.

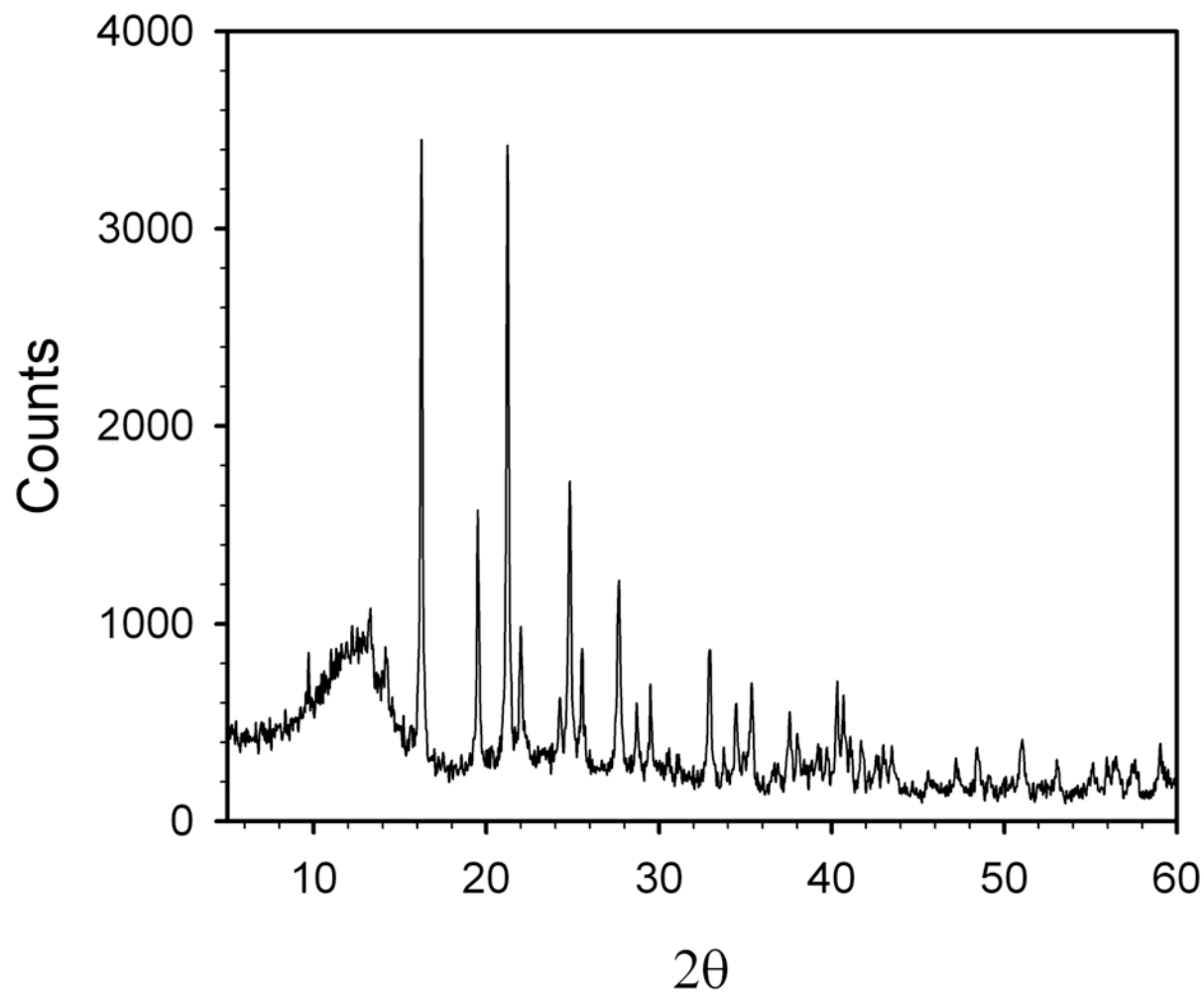


**Fig S2.** X-ray powder diffraction data for  $\text{Li}_2\text{Zn}_3[\text{Fe}(\text{CN})_6]_2 \cdot x\text{H}_2\text{O}$ . The broad peak centered at ca.  $13^\circ$  is due to scattering from the sample holder.

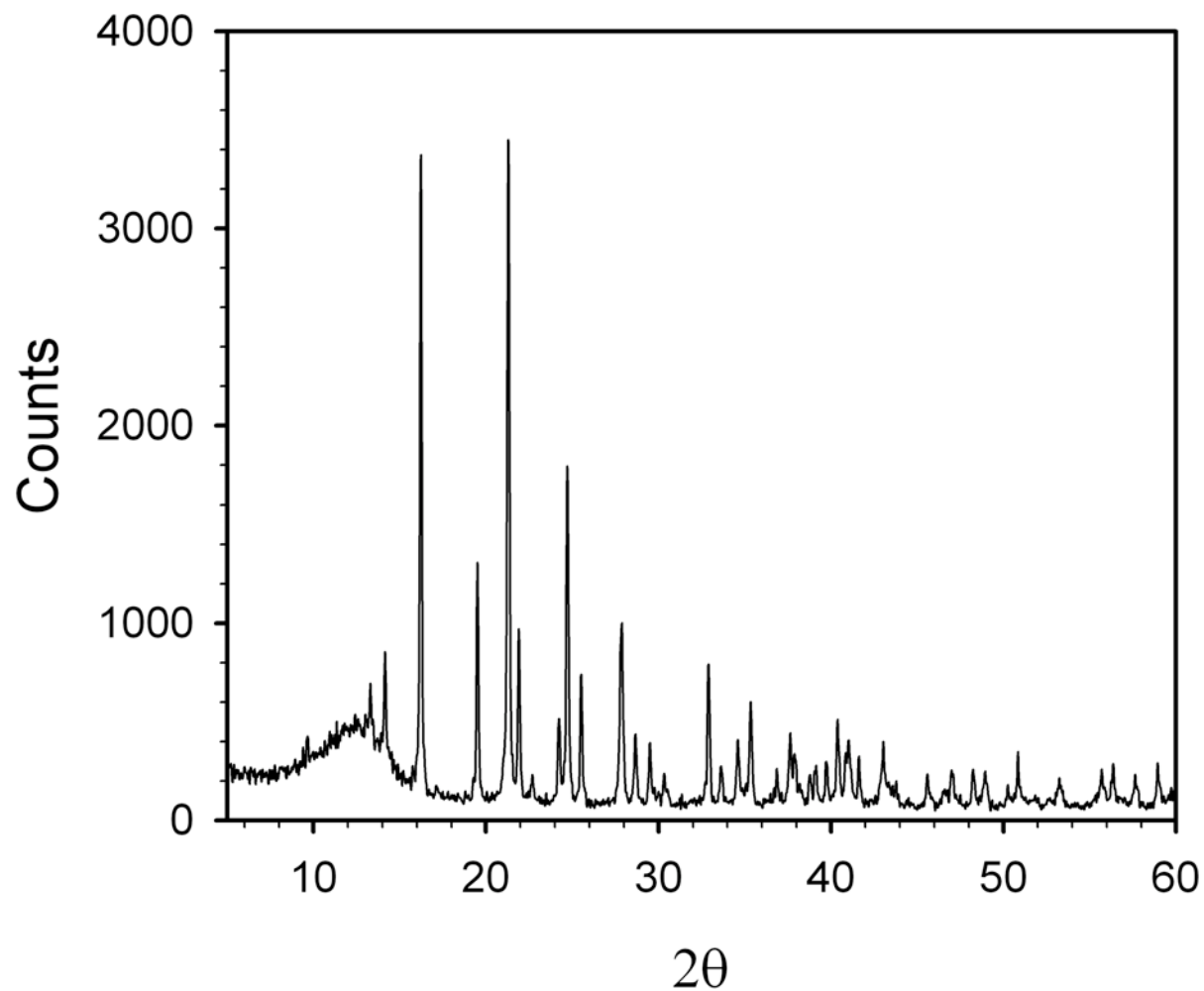


**Fig S3.** X-ray powder diffraction data for  $\text{Na}_2\text{Zn}_3[\text{Fe}(\text{CN})_6]_2 \cdot x\text{H}_2\text{O}$ . The broad peak centered at ca.  $13^\circ$  is due to scattering from the sample holder.

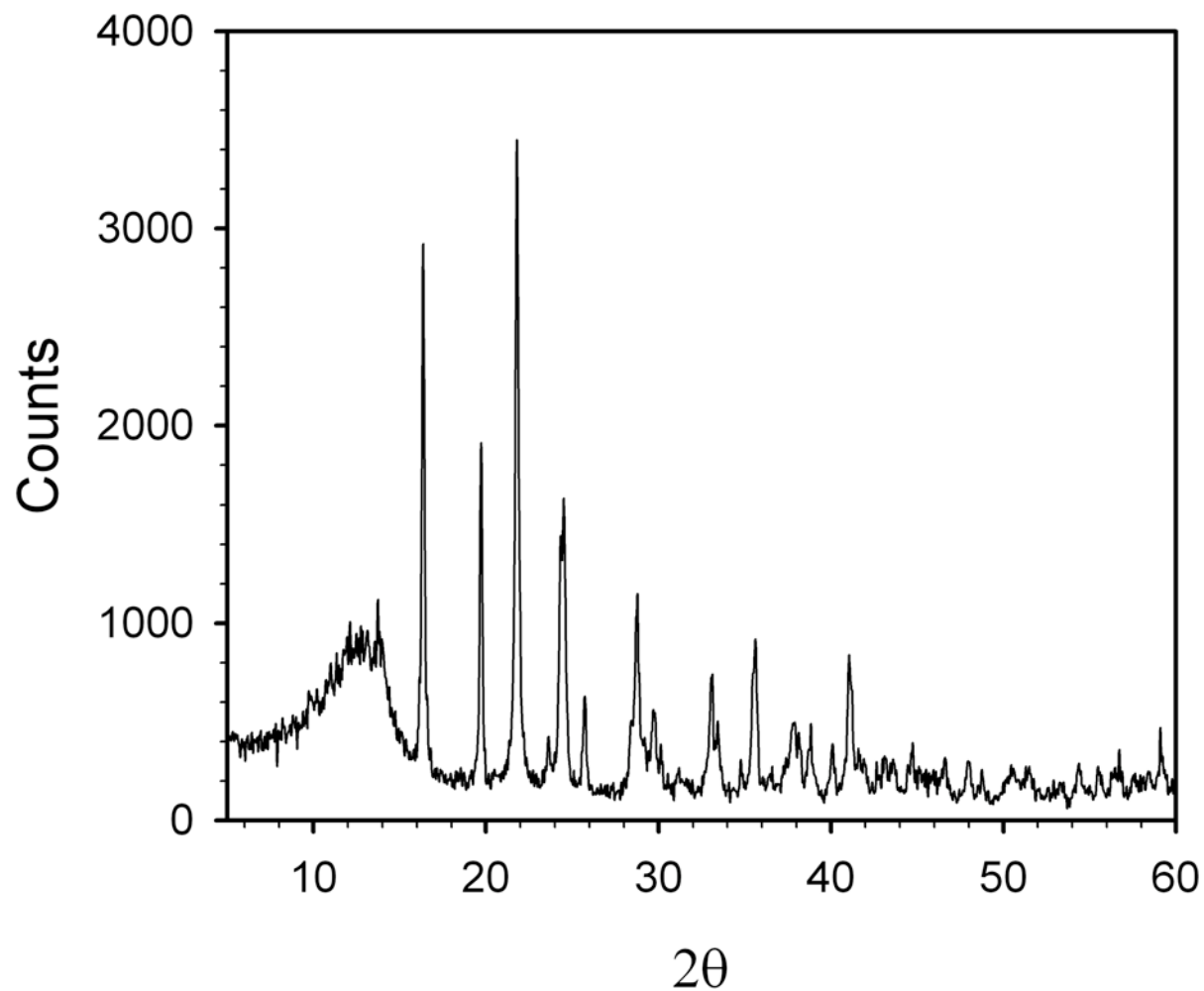


**Fig S4.** X-ray powder diffraction data for  $\text{K}_2\text{Zn}_3[\text{Fe}(\text{CN})_6]_2 \cdot x\text{H}_2\text{O}$ . The broad peak centered at ca.  $13^\circ$  is due to scattering from the sample holder.



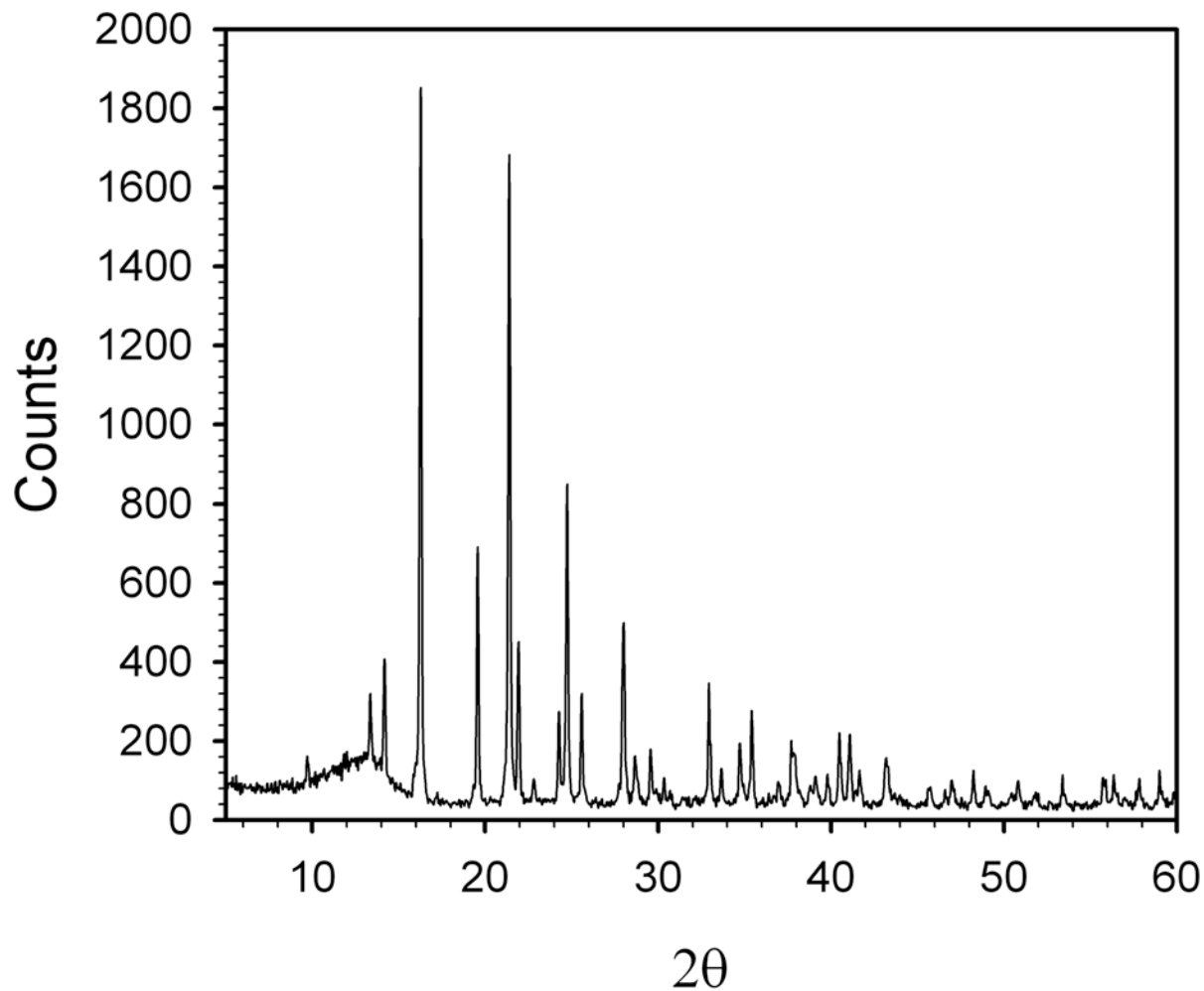


**Fig S5.** X-ray powder diffraction data for  $\text{Rb}_2\text{Zn}_3[\text{Fe}(\text{CN})_6]_2 \cdot x\text{H}_2\text{O}$ . The broad peak centered at ca.  $13^\circ$  is due to scattering from the sample holder.

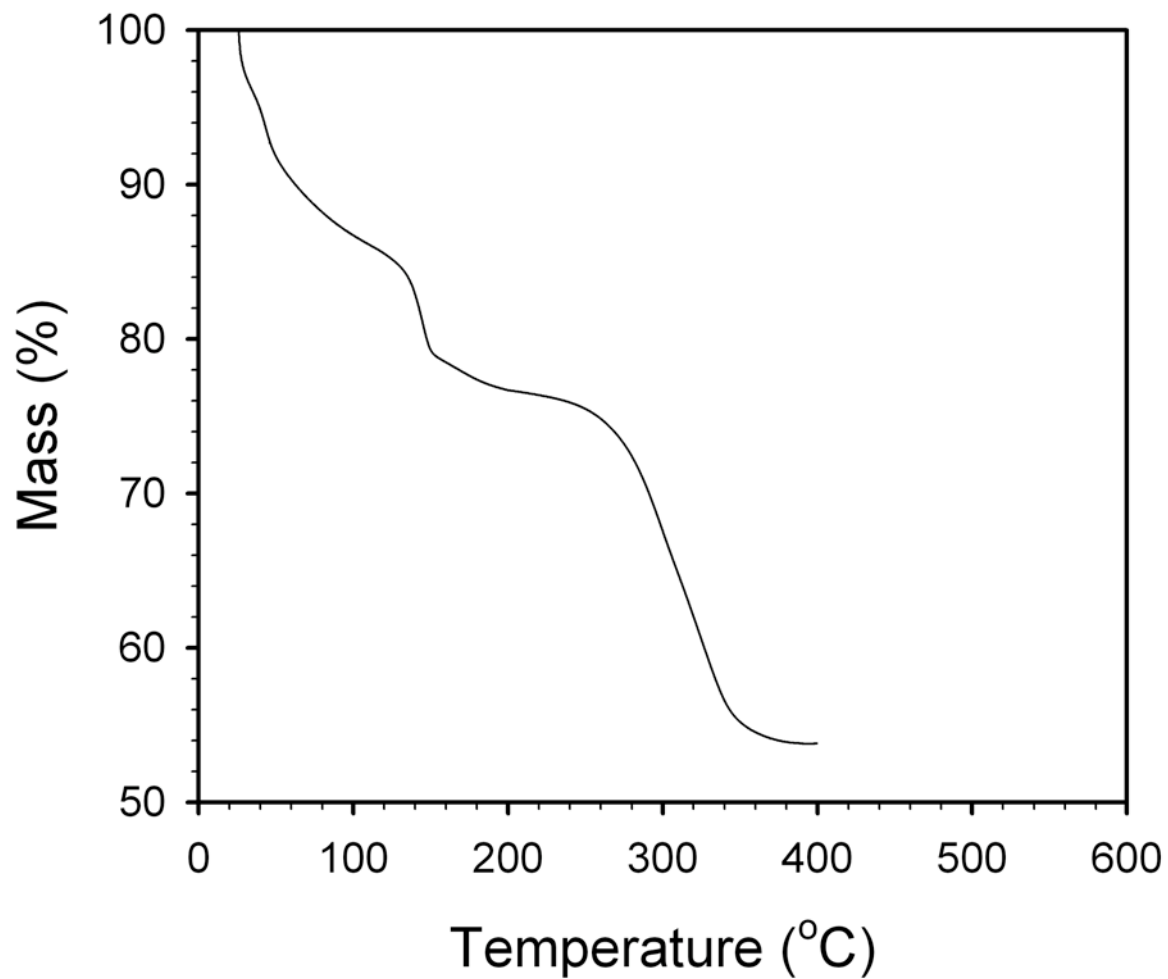


**Fig S6.** Thermogravimetric analysis showing the weight loss in  $\text{H}_2\text{Zn}_3[\text{Fe}(\text{CN})_6]_2 \cdot x\text{H}_2\text{O}$ , with temperature increasing at a rate of  $0.5\text{ }^\circ\text{C}/\text{min}$ .

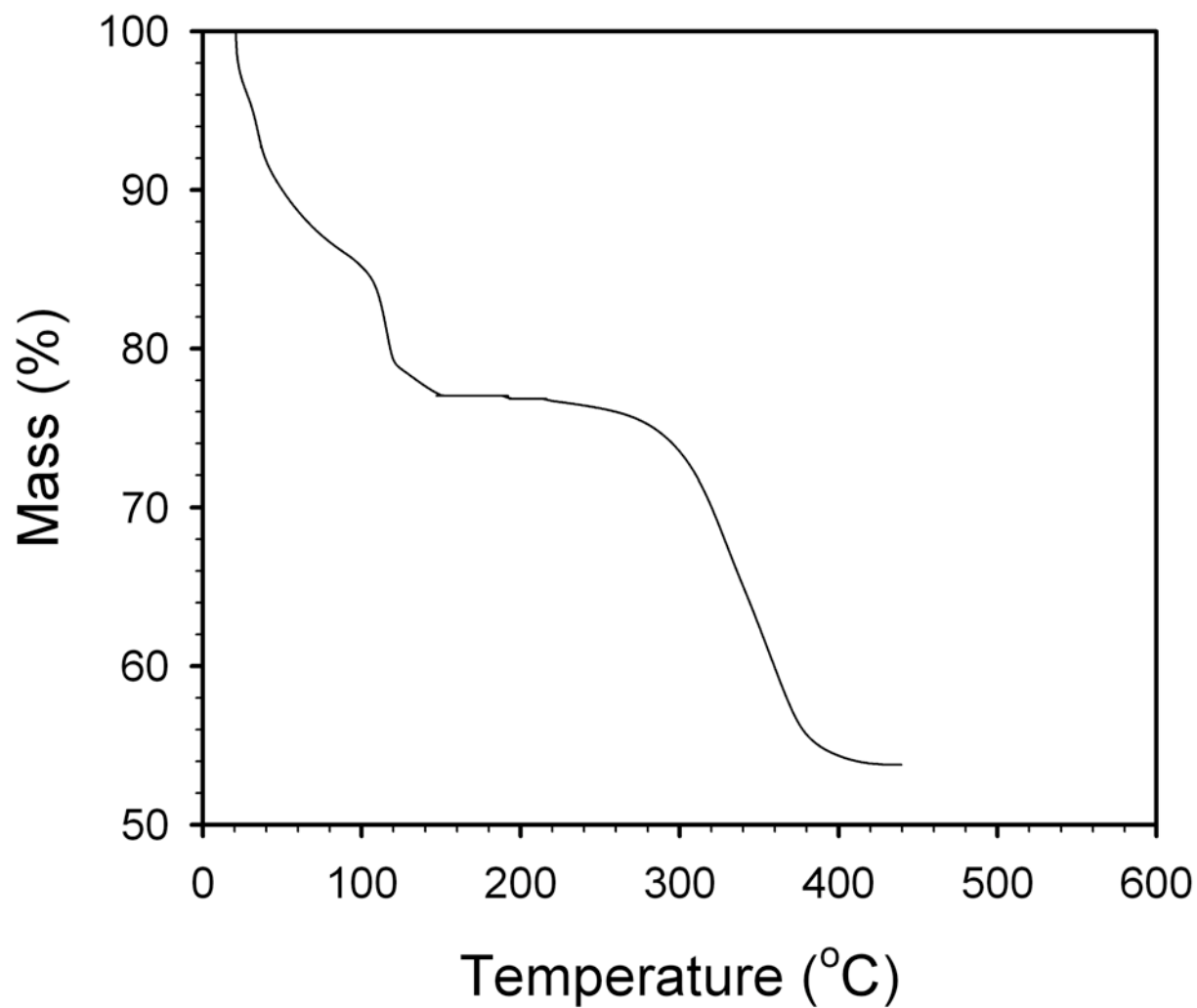


**Fig S7.** Thermogravimetric analysis showing the weight loss in  $\text{Li}_2\text{Zn}_3[\text{Fe}(\text{CN})_6]_2 \cdot x\text{H}_2\text{O}$ , with temperature increasing at a rate of  $0.5\text{ }^\circ\text{C}/\text{min}$ .

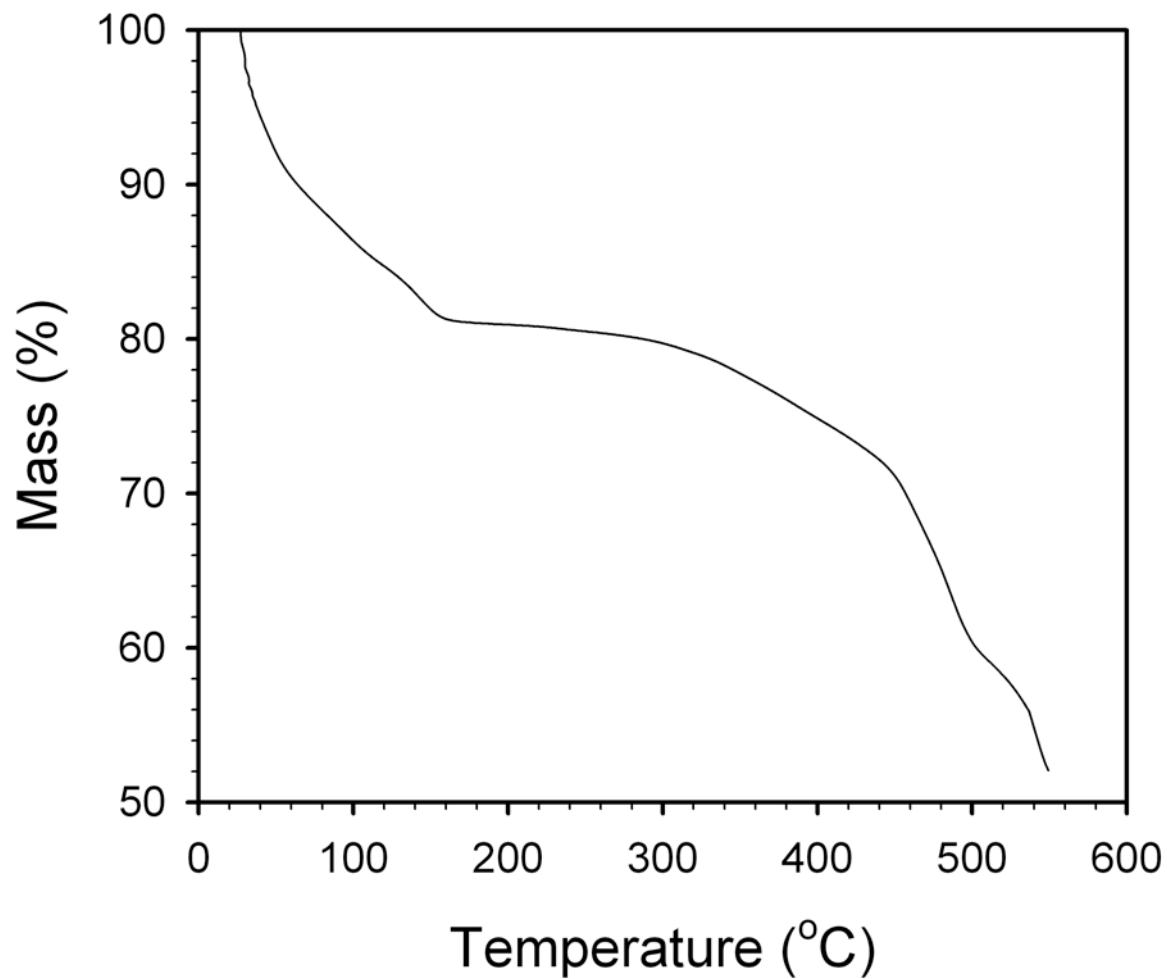


**Fig S8.** Thermogravimetric analysis showing the weight loss in  $\text{Na}_2\text{Zn}_3[\text{Fe}(\text{CN})_6]_2 \cdot x\text{H}_2\text{O}$ , with temperature increasing at a rate of  $0.5\text{ }^\circ\text{C}/\text{min}$ .

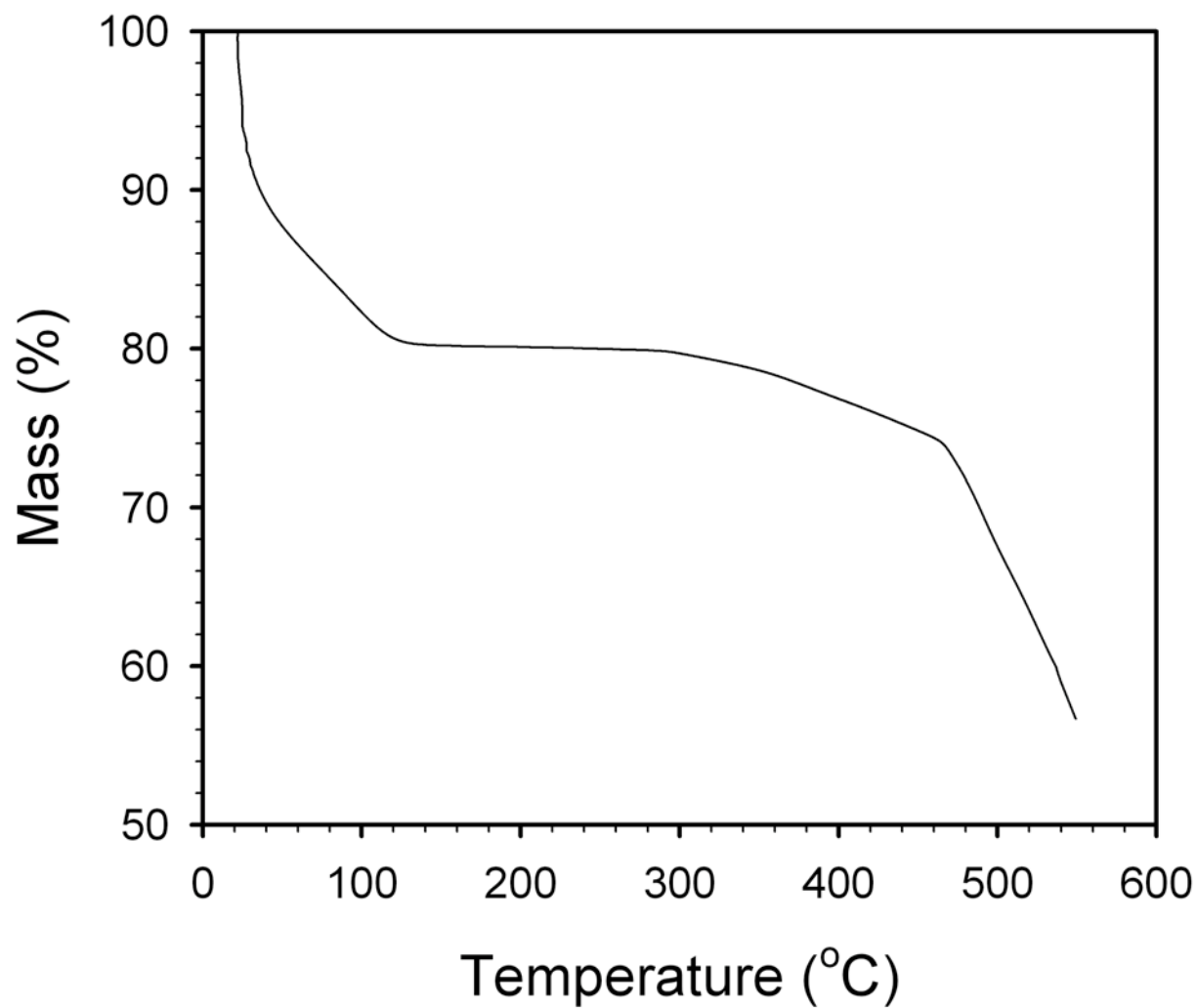


**Fig S9.** Thermogravimetric analysis showing the weight loss in  $K_2Zn_3[Fe(CN)_6]_2 \cdot xH_2O$ , with temperature increasing at a rate of 0.5 °C/min.

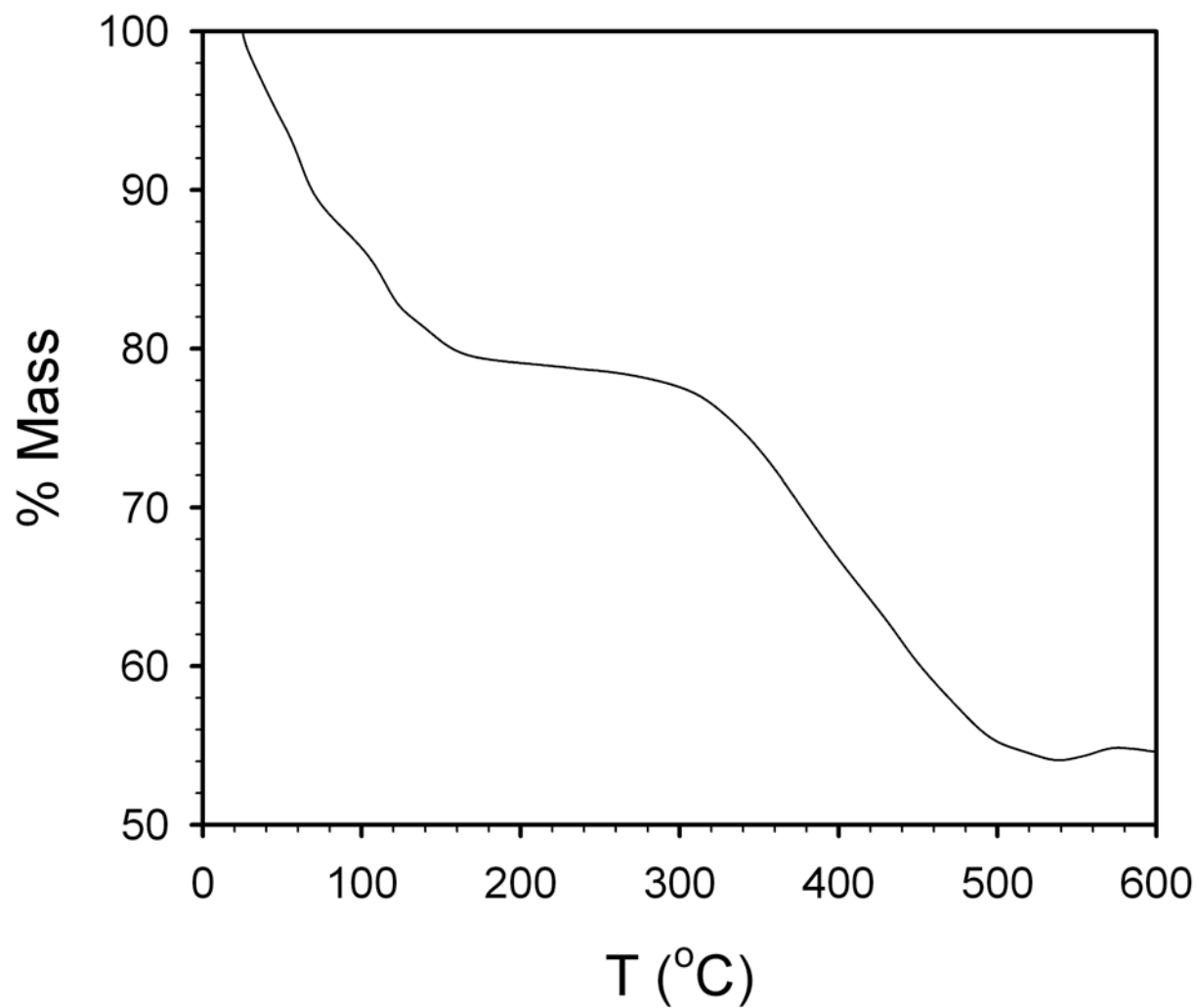


**Fig S10.** Thermogravimetric analysis showing the weight loss in  $\text{Rb}_2\text{Zn}_3[\text{Fe}(\text{CN})_6]_2 \cdot x\text{H}_2\text{O}$ , with temperature increasing at a rate of  $0.5\text{ }^\circ\text{C}/\text{min}$ .

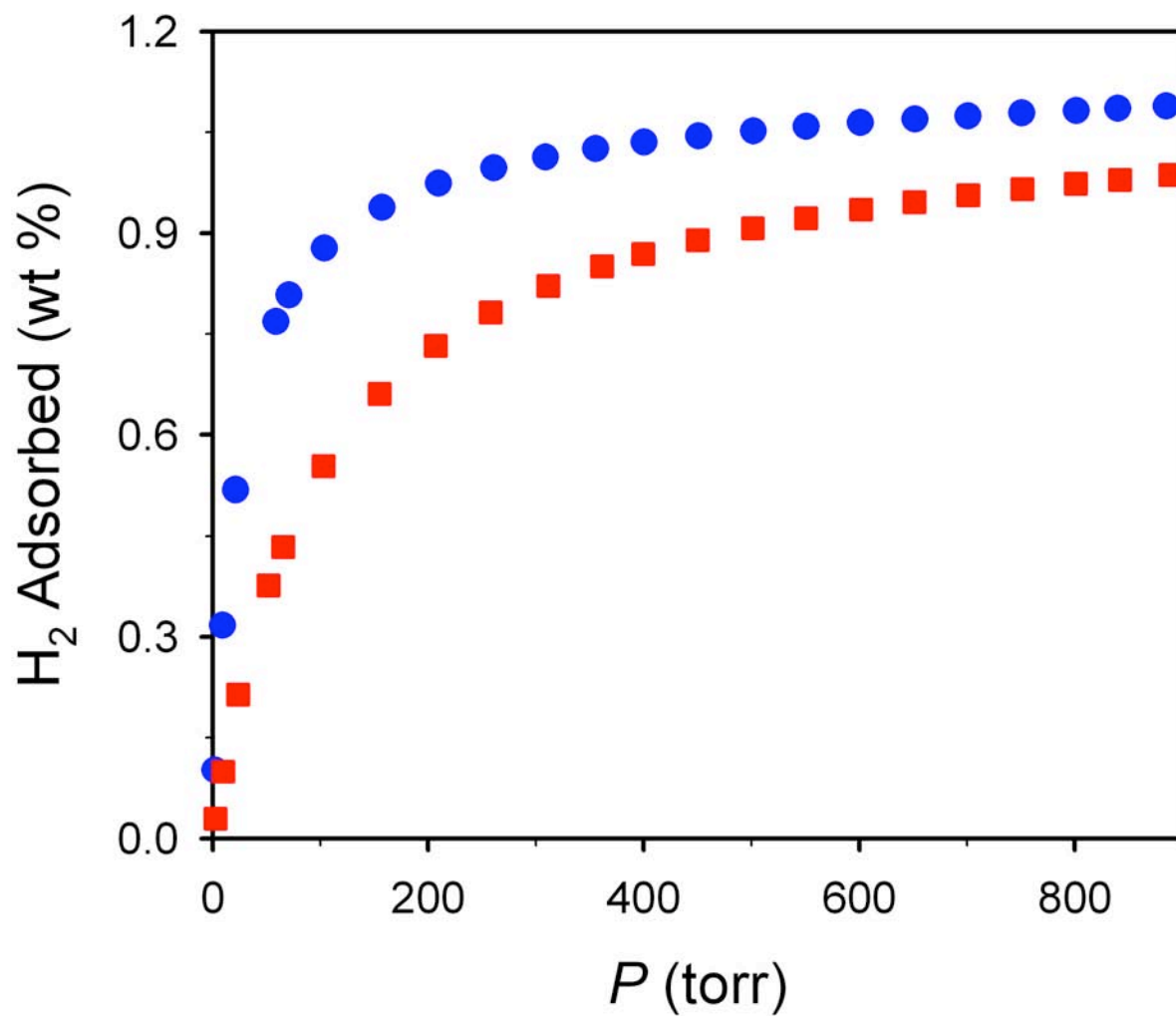


**Fig S11.** Dihydrogen adsorption isotherms for H<sub>2</sub>Zn<sub>3</sub>[Fe(CN)<sub>6</sub>]<sub>2</sub>·*x*H<sub>2</sub>O at 77 K (blue circles) and 87 K (red squares).

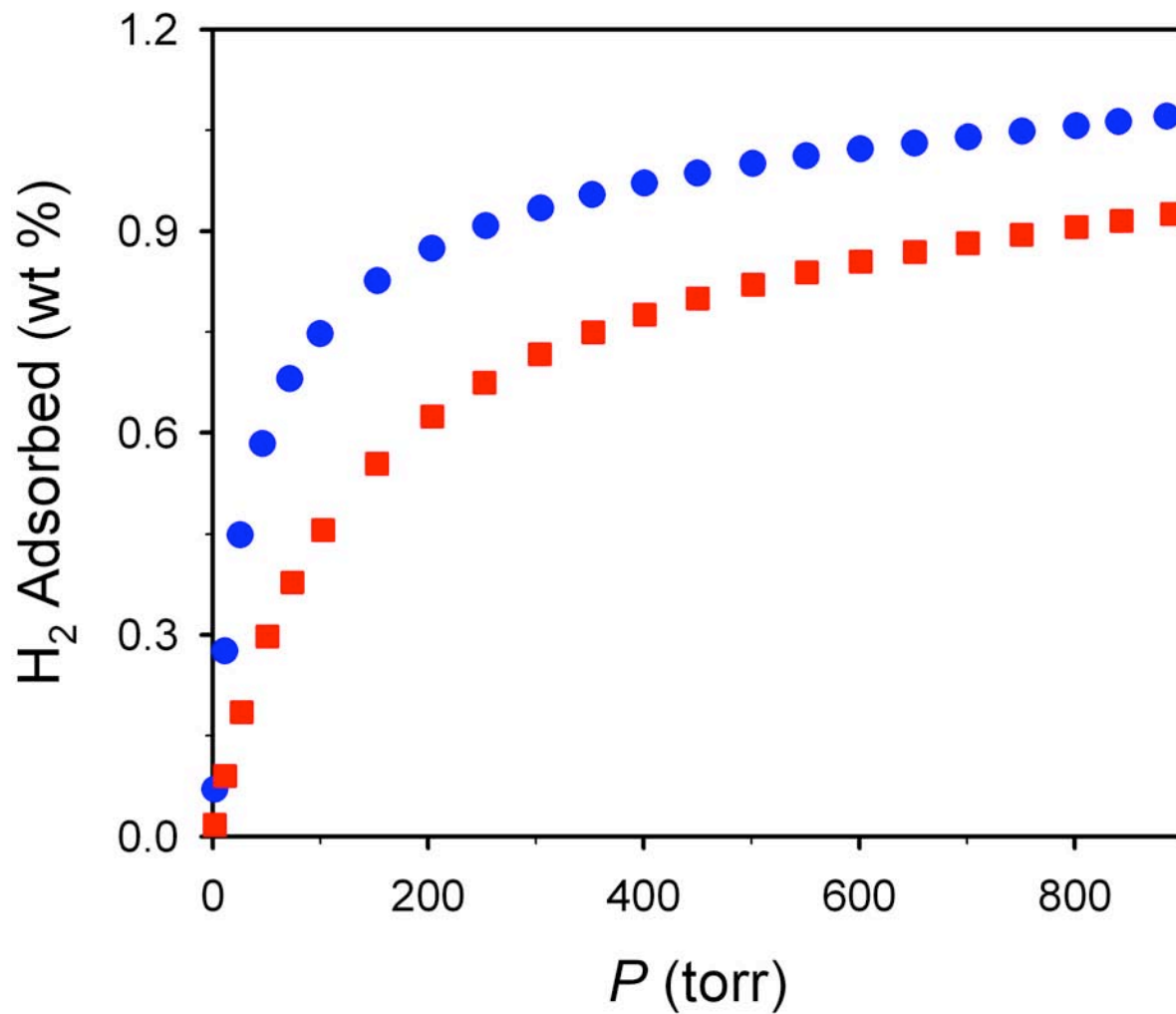


**Fig S12.** Dihydrogen adsorption isotherms for Li<sub>2</sub>Zn<sub>3</sub>[Fe(CN)<sub>6</sub>]<sub>2</sub>·*x*H<sub>2</sub>O at 77 K (blue circles) and 87 K (red squares).



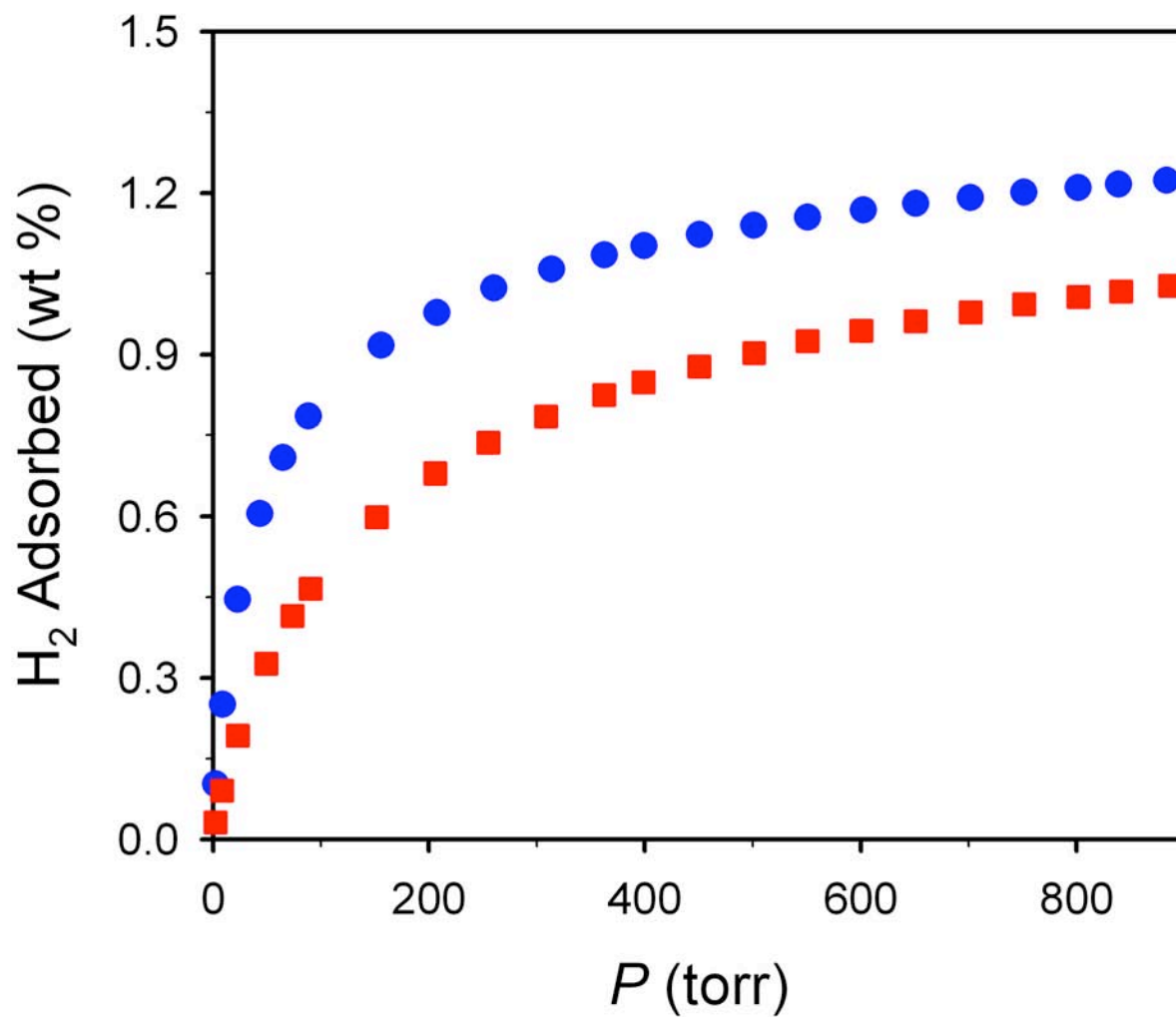


**Fig S13.** Dihydrogen adsorption isotherms for Na<sub>2</sub>Zn<sub>3</sub>[Fe(CN)<sub>6</sub>]<sub>2</sub>·*x*H<sub>2</sub>O at 77 K (blue circles) and 87 K (red squares).

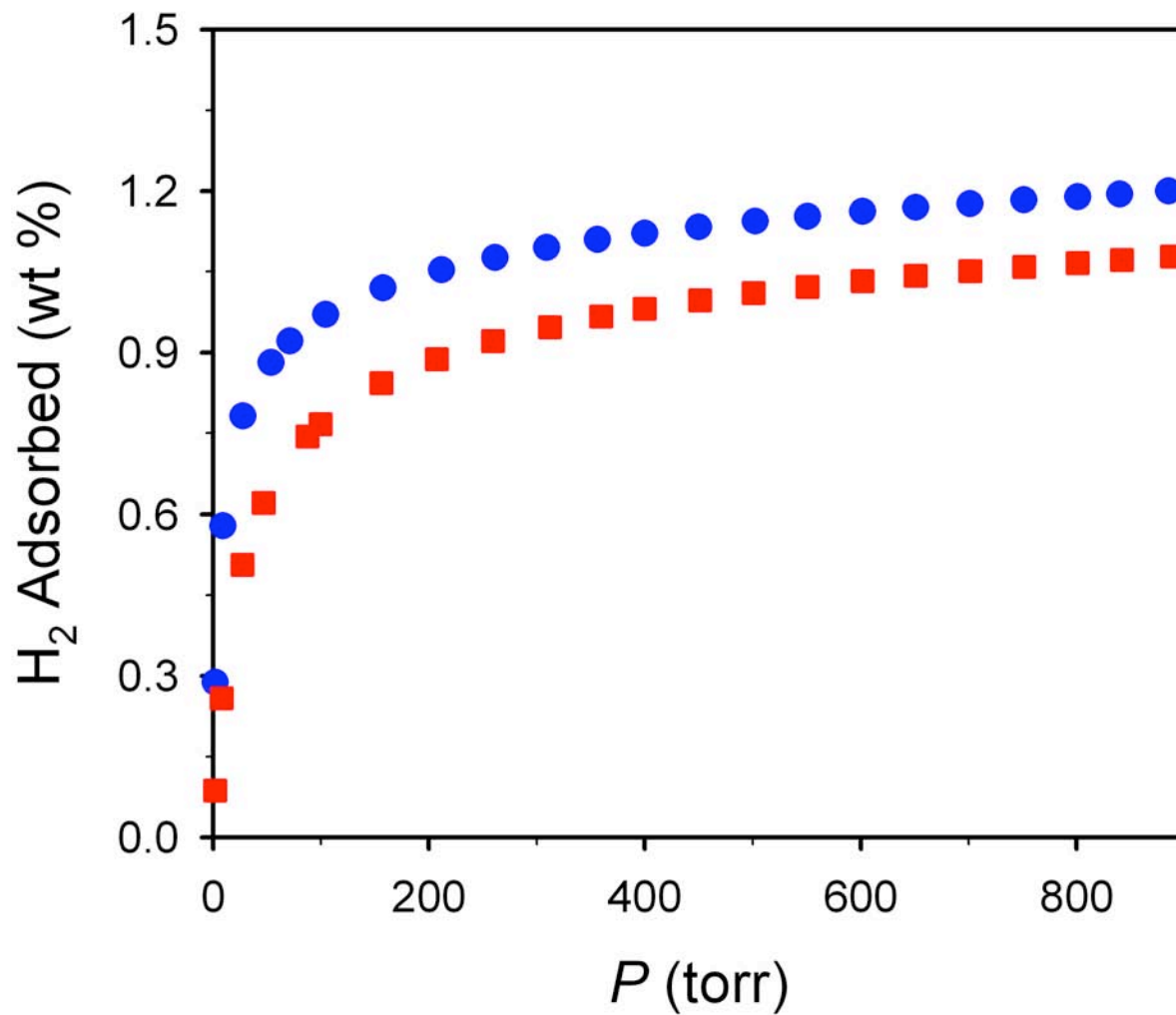


**Fig S14.** Dihydrogen adsorption isotherms for K<sub>2</sub>Zn<sub>3</sub>[Fe(CN)<sub>6</sub>]<sub>2</sub>·*x*H<sub>2</sub>O at 77 K (blue circles) and 87 K (red squares).

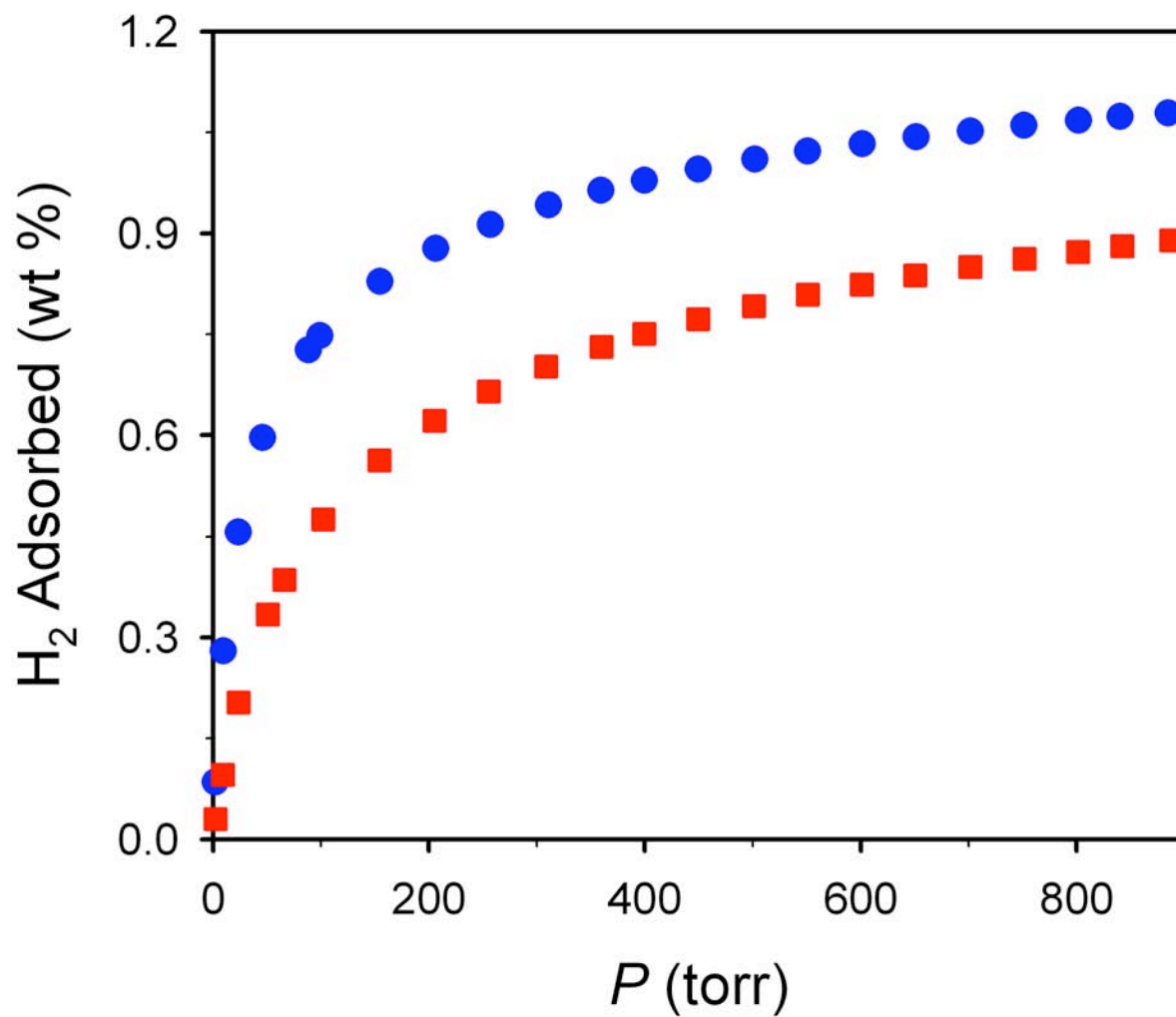


**Fig S15.** Dihydrogen adsorption isotherms for Rb<sub>2</sub>Zn<sub>3</sub>[Fe(CN)<sub>6</sub>]<sub>2</sub>·*x*H<sub>2</sub>O at 77 K (blue circles) and 87 K (red squares).

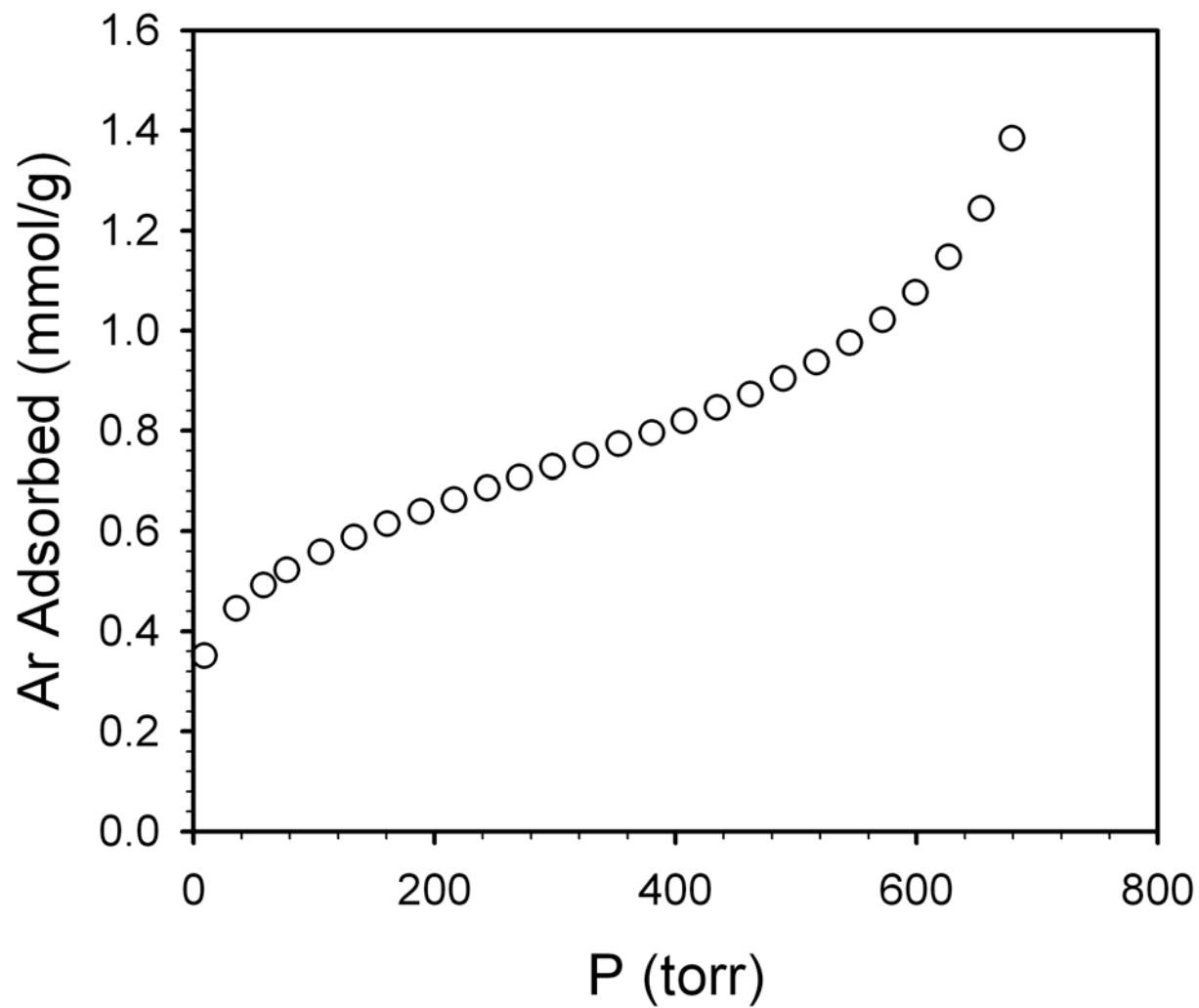


**Fig S16.** Argon adsorption isotherm for  $\text{H}_2\text{Zn}_3[\text{Fe}(\text{CN})_6]_2 \cdot x\text{H}_2\text{O}$  at 87 K.

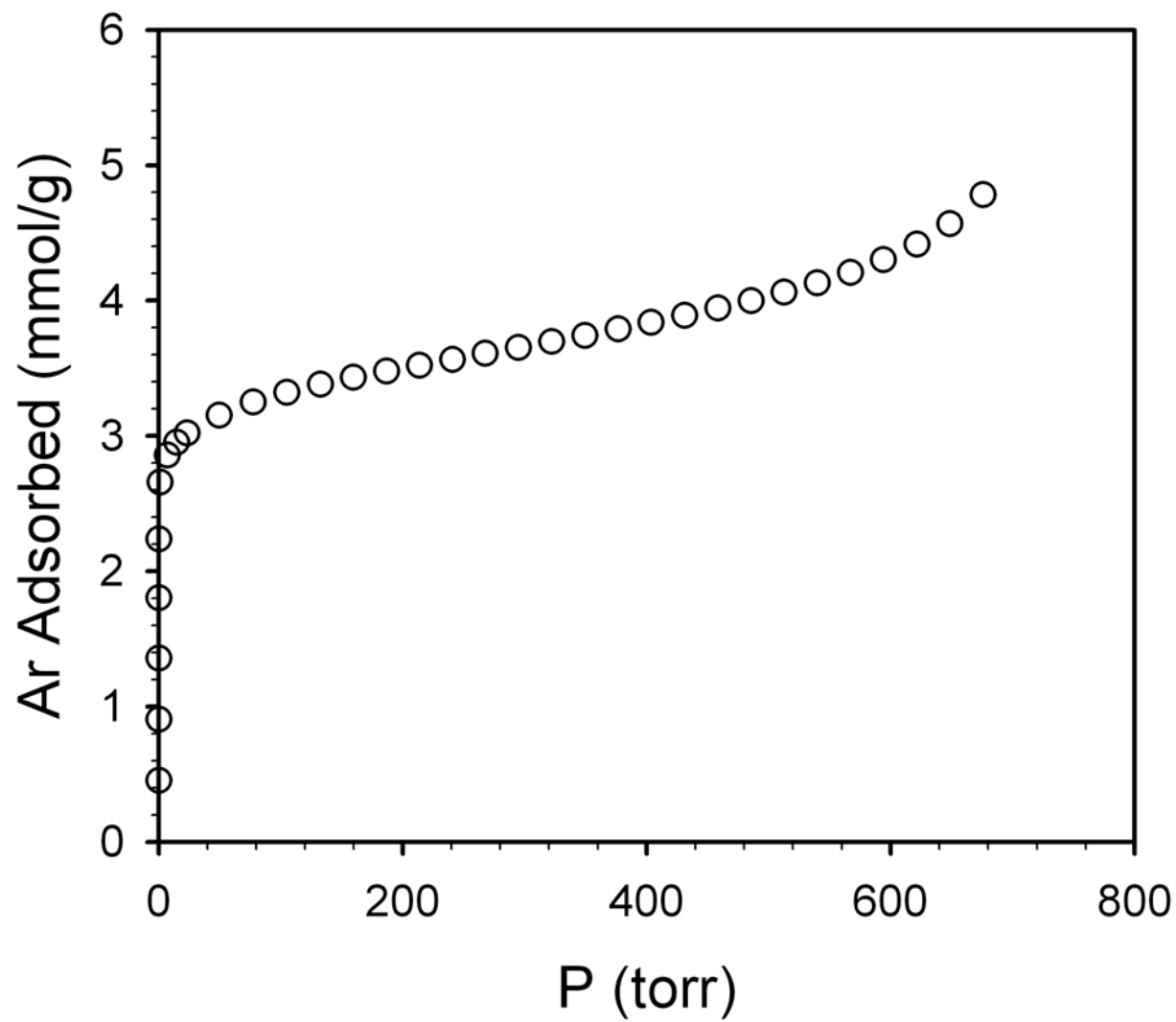


**Fig S17.** Argon adsorption isotherm for  $\text{Li}_2\text{Zn}_3[\text{Fe}(\text{CN})_6]_2 \cdot x\text{H}_2\text{O}$  at 87 K.

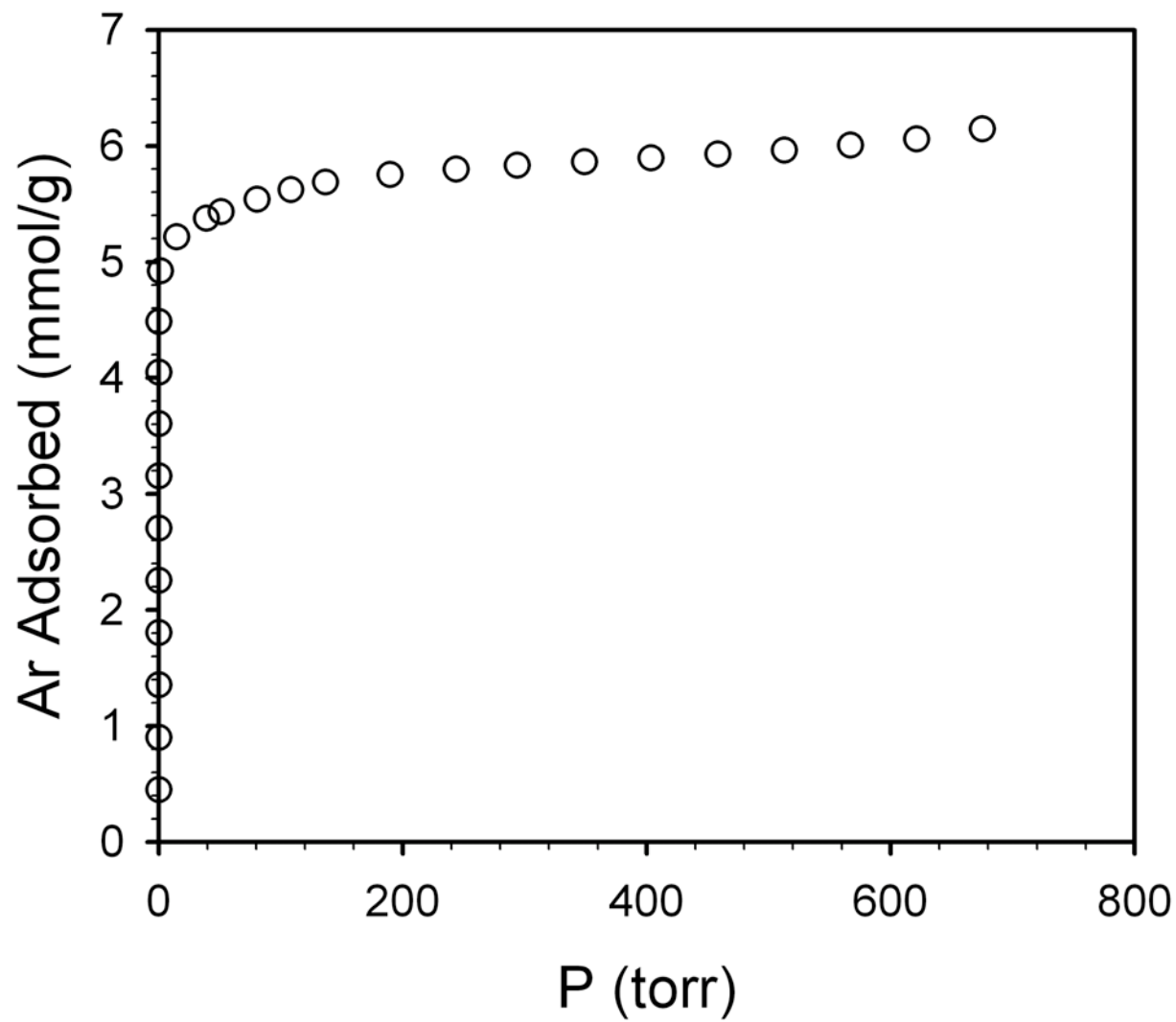


**Fig S18.** Argon adsorption isotherm for  $\text{Na}_2\text{Zn}_3[\text{Fe}(\text{CN})_6]_2 \cdot x\text{H}_2\text{O}$  at 87 K.

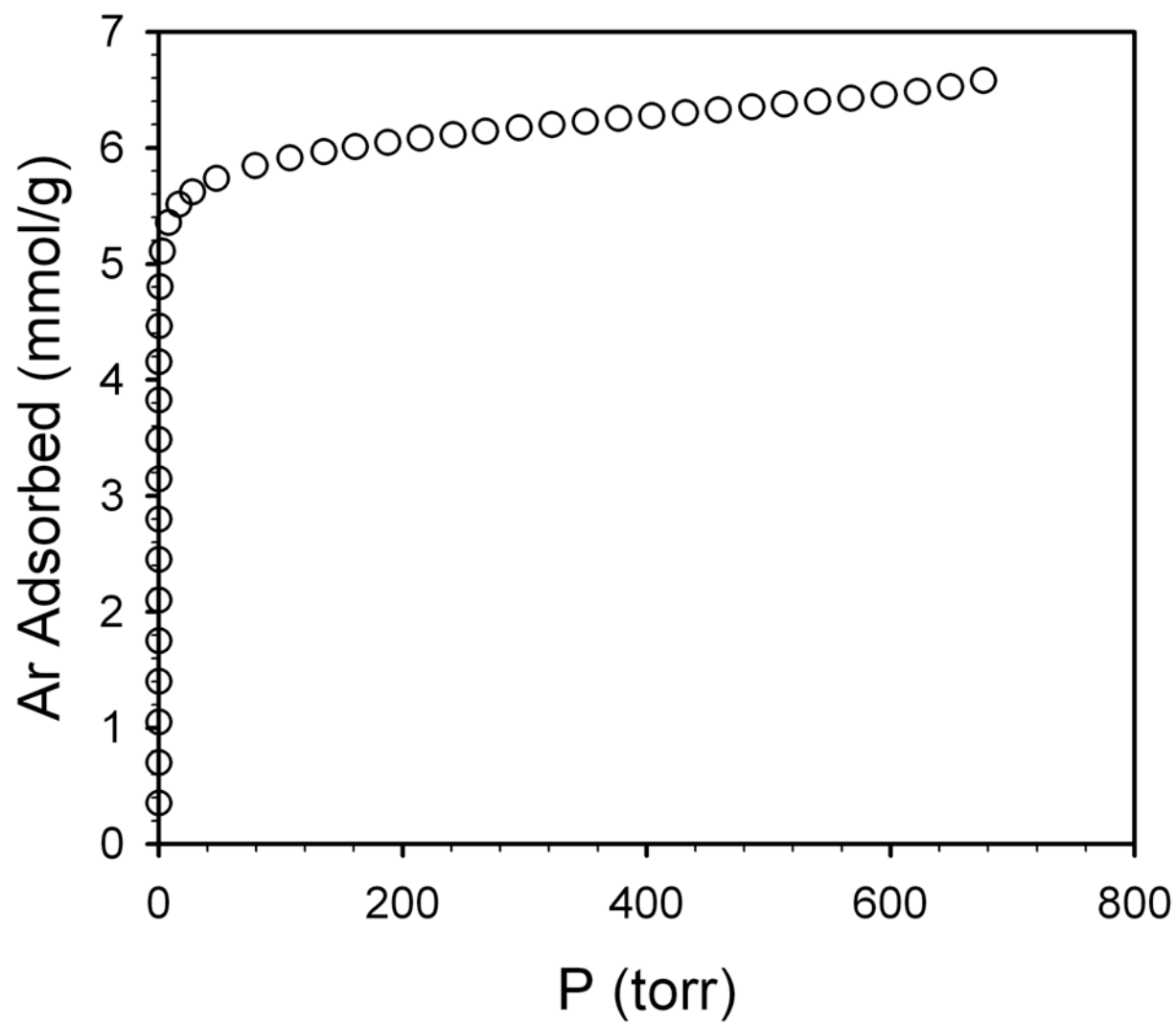


**Fig S19.** Argon adsorption isotherm for  $\text{K}_2\text{Zn}_3[\text{Fe}(\text{CN})_6]_2 \cdot x\text{H}_2\text{O}$  at 87 K.

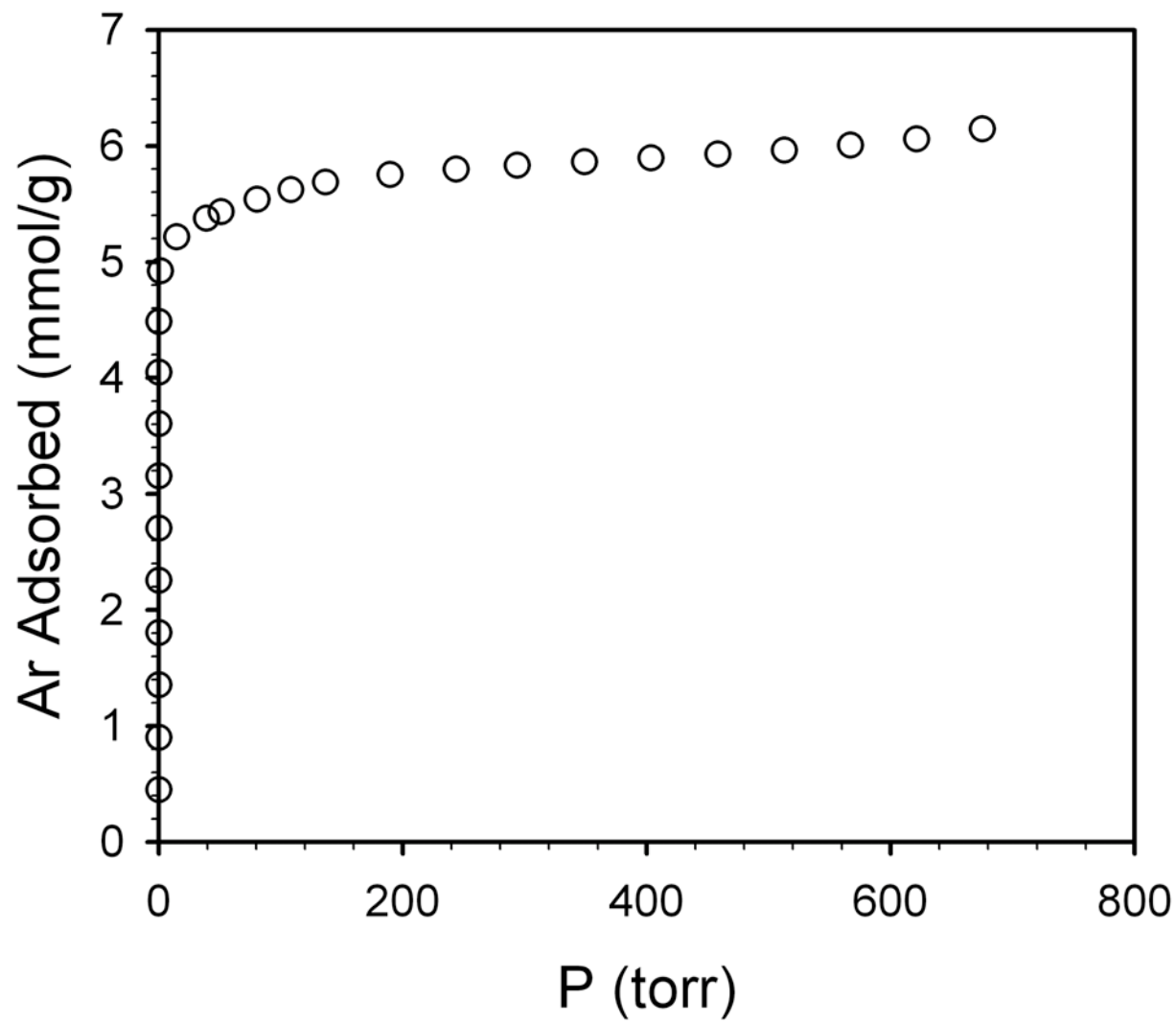


**Fig S20.** Argon adsorption isotherm for  $\text{Rb}_2\text{Zn}_3[\text{Fe}(\text{CN})_6]_2 \cdot x\text{H}_2\text{O}$  at 87 K.